AIP | Chaos
An Interdisciplinary Journal of Nonlinear Science

Pinning control of complex networks via edge snapping

P. DeLellis, M. di Bernardo, and M. Porfiri

Citation: Chaos **21**, 033119 (2011); doi: 10.1063/1.3626024
View online: http://dx.doi.org/10.1063/1.3626024
View Table of Contents: http://chaos.aip.org/resource/1/CHAOEH/v21/i3
Published by the AIP Publishing LLC.

Pinning control of complex networks via edge snapping

P. DeLellis,[1,a)] M. di Bernardo,[1,b)] and M. Porfiri[2]
[1]*Department of Systems and Computer Science, University of Naples Federico II, Naples 80125, Italy*
[2]*Department of Mechanical and Aerospace Engineering, Polytechnic Institute of New York University, Brooklyn, New York 11201, USA*

(Received 1 June 2011; accepted 27 July 2011; published online 6 September 2011)

In this paper, we propose a hierarchy of novel decentralized adaptive pinning strategies for controlled synchronization of complex networks. This hierarchy addresses the fundamental need of selecting the sites to pin through a fully decentralized approach based on edge snapping. Specifically, we present three different strategies of increasing complexity which use a combination of network evolution and adaptation of the coupling and control gains. Theoretical results are complemented by extensive numerical investigations of the performance of the proposed strategies on a set of testbed examples.
 [doi:10.1063/1.3626024]

Network synchronization can be observed in a wide range of application domains, including biology, sociology, and technology. Notably, synchronization is a common experience in human life as it is observed in metabolic processes, human interactions, and kinesiology.[1–4] Moreover, a wide spectrum of human-made devices, such as pendulum clocks, musical instruments, lasers, and power electronic systems, are characterized by prominent synchronization phenomena.[5–12] From a control viewpoint, it is typically required that the network synchronizes towards a desired trajectory generated by an exogenous dynamical system, referred to as the pinner. Control actions are applied to a limited number of network nodes, referred to as the pinned sites.[13–19] The intensity of such control actions along with the strength of the coupling among the interconnected dynamical systems are also important design parameters that determine the network synchronizability. The combined selection of all these quantities is often difficult and generally mandates complete knowledge of the network topology.[18–22] In this paper, we propose a hierarchy of novel decentralized strategies to control a network onto a desired trajectory that minimizes *a priori* knowledge of the network topology and offline control design. This hierarchy allows to adaptively evolve both the network topology through edge snapping[23] and the coupling and control gains. We perform a stability analysis of the proposed strategies to ascertain their effectiveness and inform the control design. The performance of the proposed approach is assessed on a variety of testbed examples of chaotic oscillators.

I. INTRODUCTION

Synchronization of coupled dynamical systems has been the subject of much considerable research efforts in the past two decades.[1–12,24–29] In synchronization problems, the dynamics of each network node can be represented by a nonlinear differential equation of the form $\dot{x}_i = f(x_i) + g(x_i)u_i$, where $x_i \in \mathbb{R}^n$ is the state of the i^{th} node, $u_i \in \mathbb{R}^n$ is the input that determines the interactions of the i^{th} node with its neighbors, $f : \mathbb{R}^n \to \mathbb{R}^n$ is the vector field describing the node individual dynamics, and $g : \mathbb{R}^n \to \mathbb{R}^n$ is the input function. The topology of the interconnections among these N dynamical systems can be described by a graph $\mathcal{G} = \{\mathcal{V}, \mathcal{E}\}$, where $\mathcal{V}$ is the set of vertices and $\mathcal{E}$ is the set of edges. By combining the individual dynamics with the topological interactions and an appropriate coupling protocol u_i and taking g as the identity matrix, the following network model has been developed in the late Nineties, see, for example, Refs. 5, 6, and 24–29

$$\dot{x}_i = f(x_i) + \sigma \sum_{j:(i,j)\in\mathcal{E}} (h(x_j) - h(x_i)), \qquad i = 1, \ldots, N. \quad (1)$$

Here, $h : \mathbb{R}^n \to \mathbb{R}^n$ is the output function describing the information exchanged among the network nodes and σ is the coupling strength.

From a control viewpoint, it is typically required that all the individual dynamics converge onto a desired trajectory that is denoted with $x_s(t)$, *a priori* known, and assumed to be a solution of the individual dynamics so that

$$\dot{x}_s = f(x_s). \quad (2)$$

This class of control problems finds direct application in formation control analysis of multi-vehicle teams, see, for example, Refs. 30–34. To efficiently address this control problem, so-called pinning control techniques have been introduced, see, for example, Refs. 13–19. Within these schemes, an external node, generally referred to as the "pinner," is connected only to a small fraction of the target network nodes, termed as the "pinned sites." Consequently, the equation describing the closed-loop network dynamics becomes

a)Electronic mail: pietro.delellis@unina.it.
b)Also at Department of Engineering Mathematics, University of Bristol, United Kingdom.

$$\dot{x}_i = f(x_i) + \sigma \sum_{j:(i,j)\in\mathcal{E}} (h(x_j) - h(x_i)) + \eta_i q(h(x_s) - h(x_i)),$$
$$i \in \mathcal{V}, \tag{3a}$$

$$\eta_i = \begin{cases} 1, & i = 1, \cdots, r, \\ 0, & i = r+1, \cdots, N. \end{cases} \tag{3b}$$

The convergence of all trajectories to the reference dynamics established by the pinner requires a proper selection of the coupling gain σ, the control gain q, the number of pinned sites r, and the location of such sites in the network, see, for example, Refs. 15 and 20. The selection of these quantities is often difficult and requires a thorough knowledge of the network topology, as discussed in Refs. 18–22. Typically, the nodes to be controlled are chosen offline as are the values of the coupling and control gains.

In this paper, we propose a set of novel strategies to achieve the controlled synchronization of a target network onto a desired trajectory by means of the combination of (i) network evolution (addition or removal of edges) and (ii) adaptive selection of the coupling and control gains. In particular, we propose a hierarchy of three different strategies of increasing complexity.

- "Strategy A" addresses the problem of selecting the location of the pinned sites to control a network with a static topology. The selection is performed through the edge snapping technique presented in Ref. 23.
- "Strategy B" via the controlled evolution of the network topology itself. This allows to better control nodes' dynamics, while driving the network to stable equilibrium configurations.
- "Strategy C" combines the adaptive selection of the pinning sites and the network evolution of strategy B with a modulation of the coupling and control gains, that is determined through the decentralized strategy proposed in Refs. 35 and 36.

The synergy of these strategies allows for driving the network dynamics onto the desired synchronization trajectory in a fully decentralized way in which both the nodes to be controlled and the intensity of their coupling are adaptively selected. A stability analysis of the proposed strategies is performed and complemented by extensive numerical simulations, which demonstrate that the networked dynamical systems are attracted towards locally stable equilibrium configurations. The performance of the proposed approach and the properties of the emerging topologies are investigated by focusing on a set of testbed examples.

II. PRELIMINARIES AND NETWORK MODEL

A. Mathematical preliminaries

Here, we introduce a few definitions and some notations that are used throughout the manuscript. We denote with I_d the $d \times d$ identity matrix and with 1_d the d-dimensional vector of all ones. Positive (semi-) definitiveness of a matrix A is indicated by $A > 0$ ($A \geq 0$) and negative (semi-) definitiveness by $A < 0$ ($A \leq 0$). Furthermore, we denote by $||\cdot||$ the Euclidean norm in $\mathbb{R}^n$ and its induced norm in $\mathbb{R}^{n\times n}$. Also, we define the class of k_∞ real functions[37] as follows.

Definition 2.1: A function ϕ: $[0,a) \to [0,+\infty)$ is of class k if it is continuous, strictly increasing, and $\phi(0) = 0$. It belongs to class k_∞ if the positive scalar a can be chosen to be infinitely large and $\phi(a) \to \infty$ as $a \to \infty$.

A property characterizing a nonlinear vector field is the so-called QUAD property, which is a common assumption in the literature on complex networks, see, for example, Ref. 38 and references therein. The definition of QUAD is recalled below.

Definition 2.2: A vector field $f : \mathbb{R}^n \to \mathbb{R}^n$ is said to be QUAD(Δ), if for any $x, y \in \mathbb{R}^n$

$$(x-y)^T[f(x) - f(y)] \leq (x-y)^T \Delta (x-y),$$

where Δ is an $n \times n$ diagonal matrix.

The relationship between the QUAD condition and other common assumptions on vector fields, such as contraction[39,40] and Lipschitz condition, is explored in Ref. 38.

To ease the presentation of our control strategies, we introduce a more general formulation of the network model in Eq. (3). In addition to the graph $\mathcal{G}$, associated to the topology of the target network, we define the node set $\mathcal{V}_s \subseteq \mathcal{V}$ as the set of possible pinned nodes. We introduce the following network model:

$$\dot{x}_i = f(x_i) + \sum_{j:(i,j)\in\mathcal{E}} \sigma_{ij}(t) a_{ij}(t)(h(x_j) - h(x_i)) + \eta_i(t) q_i(t)(h(x_s) - h(x_i)), \; i \in \mathcal{V}_s, \tag{4a}$$

$$\dot{x}_i = f(x_i) + \sum_{j:(i,j)\in\mathcal{E}} \sigma_{ij}(t) a_{ij}(t)(h(x_j) - h(x_i)), \quad i \notin \mathcal{V}_s, \tag{4b}$$

where $\sigma_{ij}(t)$ and $q_i(t)$ are the possibly time-varying coupling and control gains related to the link $(i,j) \in \mathcal{E}$ and the vertex $i \in \mathcal{V}_s$, respectively, and x_s satisfies Eq. (2). Also, $a_{ij}(t)$ and $\eta_i(t)$ are time-varying scalars related to $(i,j) \in \mathcal{E}$ and $i \in \mathcal{V}_s$ that are used to drive the evolution of the topology of the target network and the pinning sites' selection so that at steady-state only a portion of the links of $\mathcal{E}$ are activated and a fraction of the nodes in $\mathcal{V}_s$ are controlled. In other words, the evolution of these scalars is designed so that they are equal to 0 or 1 at steady-state. Furthermore, we define the static Laplacian matrix of the target network topology $\mathcal{L}$ whose ij^{th} entry is labelled ℓ_{ij}. Note that $\mathcal{L}$ is zero row-sum matrix whose diagonal elements correspond to the node in-degree and the off-diagonal elements are equal to -1 if $(i,j) \in \mathcal{E}$ and are 0 otherwise. Here, we study undirected graphs, that is, if $(i,j) \in \mathcal{E}$ then $(j,i) \in \mathcal{E}$. Consistently, for each network edge (i,j) or $(j,i) \in \mathcal{E}$, we consider a single coupling strength $\sigma_{ij}(t)$ and a single function $a_{ij}(t)$; in other words, the order of the subscripts in $a_{ij}(t)$ and $\sigma_{ij}(t)$ is meaningless.

With reference to Eq. (4), we define $x(t) = [x_1^T(t), \ldots, x_N^T(t)]^T$ and the pinning error of node i as $e_i = x_i - x_s$. The stack of all the pinning errors is $e(t) = [e_1^T(t), \ldots, e_N^T(t)]^T \in \mathbb{R}^{nN}$.

Notice that the network dynamics can be rewritten in term of the pinning errors as

$$\dot{e}_i = f(x_i) - f(x_s) - \sum_{j:(i,j)\in\mathcal{E}} \sigma_{ij}(t)a_{ij}(t)(h(x_i) - h(x_j)) - \eta_i(t)q_i(t)(h(x_i) - h(x_s)), \quad i \in \mathcal{V}_s, \tag{5a}$$

$$\dot{e}_i = f(x_i) - f(x_s) - \sum_{j:(i,j)\in\mathcal{E}} \sigma_{ij}(t)a_{ij}(t)(h(x_i) - h(x_j)), \quad i \notin \mathcal{V}_s. \tag{5b}$$

Throughout the paper, we consider as a reference trajectory $x_s(t)$ a bounded solution of Eq. (2), namely, a solution converging towards an equilibrium point, a limit cycle, or a chaotic attractor. We comment that even if the dynamical systems are autonomous, Equation set (5) generally describes a nonautonomous system since the reference trajectory can vary over time.

By adapting the classical definitions of stability,[37] we present the following definitions of pinning controllability.

Definition 2.3: The controlled network in Eq. (4) is said to be locally asymptotically controlled to the pinner trajectory in Eq. (2) with $t \geq 0$ if

1. For each $\varepsilon > 0$ and $t_0 \geq 0$ there exists a $\Delta_1(\varepsilon, t_0) > 0$ such that
$$\| e(t) \| < \varepsilon, \quad \forall t \geq t_0, \tag{6}$$
for $||e(t_0)|| < \Delta_1(\varepsilon, t_0)$.
2. For each $t_0 \geq 0$, there exists a constant $\Delta_2(t_0)$ such that
$$\lim_{t\to\infty} e(t) = 0, \tag{7}$$
for $||e(t_0)|| < \Delta_2(t_0)$.

Definition 2.4: The controlled network in Eq. (4) is said to be globally uniformly asymptotically controlled to the pinner trajectory in Eq. (2) with $t \geq 0$ if

1. For every $\varepsilon > 0$ there exists a $\Delta(\varepsilon) > 0$, independent of t_0, such that Eq. (6) holds for $||e(t_0)|| < \Delta(\varepsilon)$.
2. $\Delta(\varepsilon)$ can be chosen to satisfy
$$\lim_{\varepsilon\to\infty} \delta(\varepsilon) = \infty.$$
3. For each pair of positive numbers ν and c, there is a $T = T(\nu, c)$ such that
$$\| e(t) \| < \nu, \qquad \forall t \geq t_0 + T(\nu, c),$$
for $||e(t_0)|| < c$.

Definition 2.5: The controlled network in Eq. (4) is said to be globally exponentially controlled to the pinner trajectory in Eq. (2) with $t \geq 0$ if there exist positive constants c_1 and c_2 such that

$$\| e(t) \| \leq c_1 \| e(t_0) \| e^{-c_2(t-t_0)},$$

for any initial condition $x(t_0)$.

B. Network model

Controlling a complex network through pinning control requires (i) selecting the number and location of pinning sites and (ii) tuning the control gains. As noted in Ref. 15, addressing these issues through traditional approaches mandates complete knowledge of the node dynamics and of the coupling configurations. In what follows, we first assume that the coupling and control gains are fixed *a priori*. Namely, $\sigma_{ij} = \sigma \, \forall (i,j) \in \mathcal{E}$ and $q_i(t) = q \, \forall i \in \mathcal{V}_s$. We propose a novel technique to adaptively perform the selection of the pinning sites through the modulation of the scalars $\eta_i(t)$ with $i \in \mathcal{V}_s$ in Eq. (4a); this strategy is based on the concept of edge snapping introduced in Ref. 23 and referred to as strategy A. Snapping dynamics is also used in strategy B to select the steady-state topology of the target network by evolving the scalars $a_{ij}(t)$ with $(i,j) \in \mathcal{E}$. Then, we relax the assumption of fixed gains and combine the edge snapping scheme with a decentralized adaptation mechanism on the coupling and control gains $\sigma_{ij}(t)$ with $(i,j) \in \mathcal{E}$ and $q_i(t)$ with $i \in \mathcal{V}_s$ within what we term strategy C.

III. EDGE SNAPPING-BASED SELECTION OF PINNED NODES

In classical pinning control schemes, the pinned nodes are selected offline, see, for example, Eq. (3b) where they are taken to be the first r nodes. Here, inspired by the edge snapping mechanism introduced in Ref. 23 and by the work of Sĭljak,[41] we associate a dynamical system to each potential pinning edge. Hence, the selection of the pinned nodes is the result of the pinning edges' evolution. Namely, we set

$$\eta_i = b_i^2, \quad i \in \mathcal{V}_s \tag{8}$$

where the weight b_i is associated to each pinning edge and is adapted using the following second order dynamics:

$$\ddot{b}_i + \zeta \dot{b}_i + \frac{\mathrm{d}}{\mathrm{d}b_i} U(b_i) = g(\| e_i \|), \quad i \in \mathcal{V}_s. \tag{9}$$

Equation (9) represents the evolution of a unitary mass in a double-well potential U subject to an external force g which is function of the pinning error e_i and a linear damping described by ζ. In what follows, we assume that g is a smooth k_∞ function of $||e_i||$ and $\mathrm{d}g(||e_i||)/\mathrm{d}e_i$ being nought at $e_i = 0$.

A manageable selection for the potential is the following:

$$U(z) = kz^2(z-1)^2, \tag{10}$$

where k is a parameter defining the height of the barrier between the two wells. With this simple choice of the potential, the dynamical system in Eq. (9) has only two stable equilibria, namely, 0 and 1. These states correspond to the node i in $\mathcal{V}_s$ being either pinned or not, respectively.

The steady-state selection of the pinned sites, that is, the asymptotic values of η_i with $i \in \mathcal{V}_s$, is highly dependent on the initial state of the networked dynamical systems. Such initial conditions may indeed lead to a broad range of emerging pinning configurations, spanning from networks where every possible node is pinned to networks where pinning control is only applied to a single node. Therefore, a variety of coexisting

equilibrium configurations are possible. In what follows, we first focus on the local stability of these configurations. Then, we provide sufficient conditions for the network in Eq. (4) to be controlled to the desired trajectory and for the edge snapping mechanism in Eq. (9) to drive the network to a steady-state pinning configuration. The global stability of the error dynamics is addressed by assuming the vector fields of the agents are QUAD according to Definition 2.2.

A. Local pinning controllability

Imposing that all the coupling and control gains are fixed, and that $a_{ij} = 1 \forall (i,j) \in \mathcal{E}$, we can rewrite Eq. (4) as

$$\dot{y}_i = f(y_i) - \sigma \sum_{j=1}^{N+1} \mathcal{M}_{ij} h(y_j), \tag{11}$$

where $y_i = x_i$, for $i = 1,\ldots,N$, $y_{N+1} = x_s$, and $\mathcal{M}_{ij}$ is the ij^{th} element of the time-varying augmented Laplacian matrix $\mathcal{M}$ defined as

$$\mathcal{M} = \begin{bmatrix} \ell_{11} + \tilde{\eta}_1 q & \cdots & \ell_{1N} & -\tilde{\eta}_1 q \\ \vdots & \ddots & \vdots & \vdots \\ \ell_{N1} & \cdots & \ell_{NN} + \tilde{\eta}_N q & -\tilde{\eta}_N q \\ 0 & \cdots & \cdots & 0 \end{bmatrix}. \tag{12}$$

Here, we set $\tilde{\eta}_i = \eta_i$ for $i \in \mathcal{V}_s$ and $\tilde{\eta}_i = 0$ otherwise. As the target network is undirected, the matrix $\mathcal{M}$ has a real spectrum at each time instant. If we denote the eigenvalues of $\mathcal{M}$ by $\mu_i(t)$, $i = 1,\ldots, N+1$, from standard graph theory, the smallest eigenvalue μ_1 is equal to zero, $\forall t \geq 0$, see, for example, Ref. 42.

The asymptotic equilibrium configuration of the network, if achieved, is highly influenced by the initial conditions. In fact, while the unique equilibrium trajectory for the network nodes is defined by the pinner, the set $\mathcal{P}$ of possible steady-state pinning topologies has cardinality

$$\sum_{j=1}^{r} r!/j!(r-j)!,$$

where r is the number of possible pinned sites, that is, the cardinality of $\mathcal{V}_s$. These configurations comprise all the combinations of active and inactive pinning edges. Hence, we study the network local pinning controllability by considering the transverse dynamics of the networked dynamical systems and pinning edges in the neighborhood of a synchronized solution corresponding to a possible pinning configuration. In the presence of small perturbations from the pinner trajectory and from a feasible pinning configuration, we have

$$\delta\dot{y} = \left[I_{N+1} \otimes Jf(x_s) - \sigma \bar{\mathcal{M}} \otimes Jh(x_s)\right] \delta y, \tag{13a}$$

$$\delta\ddot{b}_i = -\xi \delta\dot{b}_i - 2k\ \delta b_i, \qquad i \in \mathcal{V}_s \tag{13b}$$

where the transverse dynamics is represented by $\delta y = \left[\delta y_1^T, \ldots, \delta y_N^T\right]^T$, with $\delta y_i = y_i - x_s$, and δb_i and $\delta\dot{b}_i$, $i \in \mathcal{V}_s$, represent the perturbation from the considered pinning configuration. Note that for each pinning configuration, b_i is equal to zero or unity and $\dot{b}_i = 0$ with $i \in \mathcal{V}_s$. Furthermore, $Jf(x_s)$ and $Jh(x_s)$ denote the time-varying Jacobian of f and h evaluated along the pinning trajectory, respectively, and $\bar{\mathcal{M}}$ is the time-invariant augmented Laplacian matrix associated to the considered pinning configuration. Namely, $\bar{\mathcal{M}}$ is given by Eq. (12) with values for η given by the selected pinning configuration and describes the considered equilibrium pinning topology.

Equations (13a) and (13b) are decoupled and their stability can be studied separately. In particular, Eq. (13a) can be studied by using the master stability function (MSF) approach, as shown in Refs. 20 and 43. The MSF, denoted by Λ, is given by the largest Lyapunov exponent of the coupled network and is an indicator of the transverse stability of the synchronization manifold. Given the functional form of f and h, Λ depends exclusively on the topology of the controlled network, on the pinning configuration, and on the pinning and coupling gains σ and q. Namely, Eq. (13a) is asymptotically stable if and only if $\Lambda = \Lambda(\bar{\mathcal{M}}, \sigma, q) < 0$. Of particular importance is the spectrum of $\bar{\mathcal{M}}$, that is in general complex. Let us assume that the eigenvalues $\bar{\mu}_i$ of $\bar{\mathcal{M}}$ are sorted in ascending order. The extent of the stability region, in terms of σ and q, depends solely on $\bar{\mu}_2$ and/or $\bar{\mu}_{N+1}$. In particular, if the MSF is characterized by an unbounded stability region, then its width is larger the higher $\bar{\mu}_2$ is. If the stability region is bounded, then its width decreases with the ratio $\bar{\mu}_{N+1}/\bar{\mu}_2$.

Notice that, for a given selection of f and h, and blocking the coupling and control gains, we have that Λ depends only on $\bar{\mathcal{M}}$, namely, $\Lambda = \Lambda(\bar{\mathcal{M}})$. Hence, we provide the following definition.

Definition 3.1: Given the functional form of f and h and given the coupling and control gains σ and q, we define $\mathcal{P}^* \subseteq \mathcal{P}$ the (possibly empty) subset of all possible pinning configurations such that $\Lambda(\bar{\mathcal{M}}) < 0$.

Let us assume that for the selected gains we have $\mathcal{P}^*$ non-empty. Now, we are ready to state the following theorem.

Theorem 1. *Consider any pinning configuration in $\mathcal{P}^*$. For any local perturbation, the network in Eq. (4) is locally asymptotically controlled to the pinner trajectory and the snapping dynamics in Eq. (9) is locally asymptotically stable.*

Proof. In the presence of small perturbations from the pinner trajectory and from the pinning configuration, the network dynamics can be expressed by the set of two decoupled Eq. (13). As the pinning configuration is in $\mathcal{P}^*$, we have that $\Lambda(\bar{\mathcal{M}}) < 0$ and therefore the network in Eq. (4) is locally asymptotically controlled to the pinner trajectory.

Now, consider Eq. (13b). Since ξ and k are positive coefficients, the eigenvalues of this linear homogeneous second order differential equation have negative real part. Therefore, the edge snapping dynamics is locally asymptotically stable. □

B. Global pinning controllability

Theorem 2. *If the vector field f(x) is QUAD(Δ), with $\Delta \leq \beta I_n$, for some $\beta < 0$, and the output function is of the form $h(x_i) = \Gamma x_i$, with $\Gamma \geq 0$, then*

- *The network in Eq. (4) is globally exponentially controlled to the desired trajectory described by Eq. (2).*

- *The dynamics of the selection of the pinned sites described by Eq. (9) converges to an equilibrium configuration where nodes are either pinned or not pinned.*

Proof. First, we prove that the error trajectories asymptotically converge to zero. Consider the classical Lyapunov function

$$V(e) = \frac{1}{2} e^T e. \tag{14}$$

From Eq. (5), we have that its derivative along the error trajectories of the system is given by

$$\dot{V} = \sum_{i=1}^{N} e_i^T (f(x_i) - f(x_s)) - \sum_{i=1}^{N} e_i^T \sigma \sum_{j=1}^{N} \ell_{ij} h(e_j) - \sum_{i \in \mathcal{V}_s} \eta_i q e_i^T h(e_i). \tag{15}$$

From Definition 2.2, it is easy to show that

$$\dot{V} \leq e^T (I_N \otimes \Delta) e - \sigma \sum_{i=1}^{N} \sum_{j=1}^{N} \ell_{ij} e_i^T h(e_j) - \sum_{i \in \mathcal{V}_s} \eta_i q e_i^T h(e_i). \tag{16}$$

Considering that $h(x_i) = \Gamma x_i$, we can write

$$\dot{V} \leq e^T (I_N \otimes \Delta) e - \sigma e^T (\mathcal{L} \otimes \Gamma) e - q e^T (E \otimes \Gamma) e, \tag{17}$$

where $E = \mathrm{diag}(\eta_1, \ldots, \eta_N)$. Since $\mathcal{L} \otimes \Gamma \geq 0$ and $E \otimes \Gamma \geq 0$ and using Eq. (8), we find

$$\dot{V} \leq \beta e^T e. \tag{18}$$

Hence, the network in Eq. (3) is globally exponentially controlled to the desired trajectory.

Now, consider Eq. (9) describing the adaptive pinning sites selection. By selecting the form of the potential in Eq. (10), Eq. (9) corresponds to a Duffing-Holmes oscillator, first introduced in Ref. 44 to model a buckled beam undergoing forced lateral vibrations. Differently from Ref. 44, the forcing is not periodic and it is rather a k_∞ function of the error norm. Since the error norm is exponentially decreasing, we can conclude that the forcing asymptotically vanishes. Furthermore, since Eq. (10) is sufficiently smooth, for $i \in \mathcal{V}$ we have that as $b_i \to +\infty$, $\ddot{b}_i \to -\infty$ with a cubic power growth. Hence, each b_i is upper bounded. Similar arguments can be used to show that each b_i is lower bounded for $i \in \mathcal{V}_s$. Then, each b_i converges to one of its equilibria, namely $b_i^\infty \in \{0, 1/2, 1\}$ for $i \in \mathcal{V}_s$. As explained above, by linearizing in the neighborhood of each equilibrium, it is easy to show that 0 and 1 are stable equilibria corresponding to the wells of the potential, while $1/2$ is unstable. Hence, if we exclude trivial cases, the pinning configuration evolves to a steady-state configuration, whose structure depends on the initial conditions and on the design of the parameters ζ and k in Eqs. (9) and (10). □

Remark. The above result provides a sufficient condition for global pinning controllability of the network. The assumption on the vector field is clearly satisfied by asymptotically stable linear time invariant systems. Notice that the QUAD assumption does not require that the vector field is continuous and therefore can be satisfied also by piecewise continuous systems. Examples of continuous QUAD systems include Lipschitz systems and C^1 systems with bounded Jacobian, see Ref. 38 for further discussion. We observe that even if the QUAD assumption with β negative may appear overly restrictive, it guarantees stability of the overall closed loop error dynamics despite the time-varying state-dependent nature of the underlying network structure. The condition of β negative may be relaxed by introducing additional hypothesis on the selection of the pinned sites. Specifically, by enforcing that at least one site is always pinned, the condition in Ref. 15 can be adapted to bound the right hand side of Eq. (16) by a negative quadratic term in the error.

C. Numerical examples

To show the effectiveness of this approach, we consider two testbed examples, where we select the forcing of potential in Eq. (10) to be $g(||e_i||) = ||e_i||^2$. We first consider a network of Chua's circuits and we then analyze a network of Lorenz oscillators.

1. Network of Chua's circuits

The equations describing the isolated circuit can be written as

$$\begin{aligned} \dot{v} &= \xi_1(-w - \gamma(v)), \\ \dot{w} &= v - w + z, \\ \dot{z} &= \xi_2 w, \end{aligned}$$

where $x = [v,w,z]^T$ is the state of the system and $\gamma(v) = m_0 v + \frac{1}{2}(m_1 - m_0)(|v+1| - |v-1|)$. The circuit parameters are $\xi_1 = 4.92$, $\xi_2 = 3.64$, $m_0 = -0.07$, and $m_1 = 1.5$, see Ref. 45. This parameter selection induces chaotic behavior, as reported in Ref. 45.

In our simulation, we consider a target network of 100 Chua's circuits linearly coupled through all the state vector in the form $h(x) = x$. The initial condition for the pinner is selected to be $x_s(0) = [0.5, 0.5, 0.5]^T$, while the initial conditions in the target network are taken from a uniform distribution between 0.5 and 1.5. The topology of the target network is scale-free like and is generated randomly by using the Barabàsi-Albert algorithm.[46] Furthermore, we take $\sigma = 0.1$, the control gain q is set to 20 and $\mathcal{V}_s = \mathcal{V}$. The aim of the control is to synchronize all nodes of the target network to the dynamics of the pinner. As reported in Figure 1, the error dynamics rapidly converge to zero, while the pinning configuration slowly converges to an equilibrium where 41 nodes are pinned. This behavior is in agreement with Theorem 1 since we have that $\Lambda(\bar{\mathcal{M}})$ is negative at the final equilibrium configuration.

2. Network of Lorenz oscillators

Here, we consider a network of 100 Lorenz oscillators[47–49] coupled through a Erdös and Rényi (ER) random

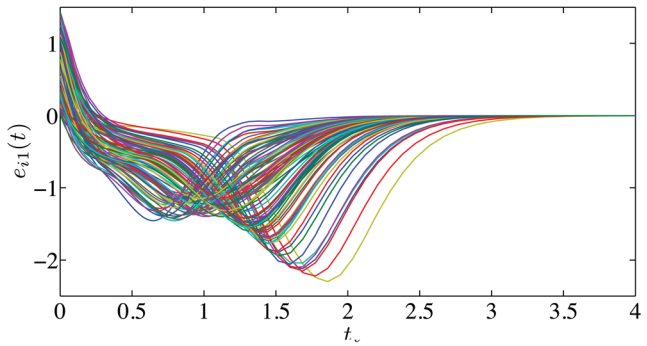

(a) Evolution of the first component of the pinning error.

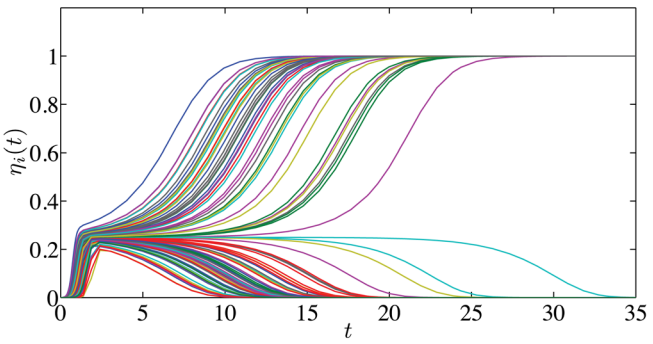

(b) Evolution of $\eta_1, \ldots, \eta_N$.

FIG. 1. (Color online) Pinning control via edge snapping in a network of 100 Chua's circuits with fixed control gains.

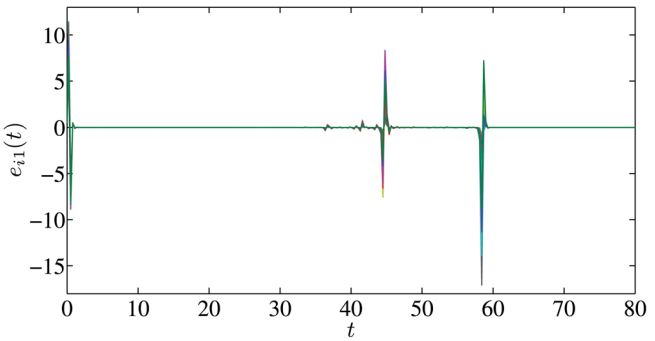

(a) Evolution of the first component of the pinning error.

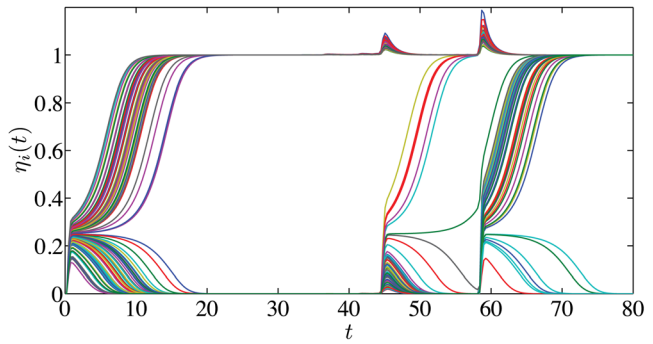

(b) Evolution of $\eta_1, \ldots, \eta_N$.

FIG. 2. (Color online) Pinning control via edge snapping in a network of 100 Lorenz oscillators with fixed control gains.

graph.[50] The dynamics of an isolated node is described by the following set of three coupled differential equations:

$$\dot{v} = a_1(w - v),$$
$$\dot{w} = a_2 v - w - vz,$$
$$\dot{z} = vw - a_3 z,$$

where $x = [v, w, z]^T$ is the state vector and $a_1 = 10$, $a_2 = 28$, and $a_3 = 8/3$. Moreover, we assume that the oscillators are diffusively coupled on all the three variables, namely, $h(x) = x$. The initial conditions on the target network nodes are taken from a uniform distribution between 0.5 and 3, while the initial conditions for the pinner are $x_s(0) = [0,1,2]^T$. We further assume that the target network is weakly coupled so that $\sigma = 0.01$, $\mathcal{V}_s = \mathcal{V}$, and the control gain q is equal to 40.

As we observe from Figure 2, at the onset of the evolution, the snapping dynamics initiates and the pinning error is suddenly reduced; while after time $t = 20$, only a small fraction of the network nodes is pinned, namely, 36 over 100. Nonetheless, this fraction is not enough to control the network: at time $t = 44$ and $t = 59$, we observe two bursts in the error dynamics. The snapping dynamics is able to immediately react to the sudden increase of the pinning error, deciding to pin another fraction of the network nodes, for a total of 81 pinned nodes. This leads the network to a stable controlled trajectory characterized by a negative value of $\Lambda(\bar{\mathcal{M}})$.

IV. TOPOLOGICAL CONTROL OF NETWORKS

Here, we relax the assumption of a static target network used in Sec. II. We consider evolving the topology of the target network towards a steady-state configuration to enhance its controllability. To this aim, we formulate strategy B as the combination of the adaptive pinning selection introduced in Sec. III with the adaptive evolution of the network topology itself. Specifically, we assume that each potential edge among the nodes in the target network is associated to a snapping dynamics. Namely, we set

$$a_{ij} = \alpha_{ij}^2, \qquad (i,j) \in \mathcal{E}, \tag{19}$$

where the weight α_{ij} is associated to every undirected edge of the target pinning edge and is adapted using the following second order dynamics

$$\dot{\alpha}_{ij} + \nu\dot{\alpha}_{ij} + \frac{\mathrm{d}}{\mathrm{d}\alpha_{ij}} U(\alpha_{ij}) = c(||e_{ij}||), \qquad (i,j) \in \mathcal{E}, \tag{20}$$

where $e_{ij} = e_j - e_i$ and we select the same potential as in Eq. (10). Furthermore, we assume that c is a smooth k_∞ function of $||e_{ij}||$, see Definition 2.1, such that $\mathrm{d}c(||e_{ij}||)/\mathrm{d}e_{ij}$ is nought at $e_{ij} = 0$. Therefore, the target network topology evolves in a decentralized way; the local mismatch of the trajectories acts as an external forcing on the edge dynamics, inducing the activation of the corresponding connection. We describe this evolving topology through the matrix $\tilde{\mathcal{L}}$ than can be assimilated to a Laplacian matrix of a time-varying weighted graph

$$\tilde{\ell}_{uv} = \begin{cases} \sum_{j:(u,j)\in\mathcal{E}} a_{uj} & \text{if } u = v, \\ -a_{uv} & \text{if } (u,v) \in \mathcal{E} \\ 0 & \text{otherwise.} \end{cases} \tag{21}$$

Note that such time-varying Laplacian shares the same nought elements as the static Laplacian $\mathcal{L}$ since the proposed

evolution only acts on the links in $\mathcal{E}$, that is, on the nonzero elements of $\mathcal{L}$ that can be turned from -1 to 0 through edge snapping.

By adopting the above topological control scheme, the stability results described in Sec. III C 2 can be easily extended as follows.

Theorem 3. *If the vector field f is QUAD(Δ), with* $\Delta \leq \beta I_n$, $\beta < 0$, *and the output function is of the form* $h(x_i) = \Gamma x_i$, *with* $\Gamma \geq 0$, *then*

- *The network in Eq. (4) is globally exponentially controlled to the desired trajectory described by Eq. (2).*
- *The dynamics of the selection of the pinned sites described by Eq. (9) converges to an equilibrium configuration where nodes are either pinned or not.*
- *The evolution of the edges of the target network described by Eq. (20) converges to an equilibrium configuration.*

Proof: The stability proof follows the same line of arguments as in Theorem 2. □

When the assumptions in Theorem 3 are not fulfilled, the error dynamics may still be locally stable. Before giving our result on local stability, we need to make some preliminary considerations. The network dynamics can be described by Eq. (11) upon substituting $\mathcal{L}$ with $\tilde{\mathcal{L}}$ in the matrix $\mathcal{M}$, see Eq. (12). To assess local stability, we consider the transverse dynamics of each node and the dynamics of the displacements from the equilibrium configurations of the target and pinning networks. Thus, we obtain

$$\delta\dot{y} = \left[I_{N+1} \otimes Jf(x_s) - \sigma\bar{\mathcal{M}} \otimes Jh(x_s)\right]\delta y, \tag{22a}$$

$$\delta\ddot{b}_i = -\xi\delta\dot{b}_i - 2k\ \delta b_i, \qquad i \in \mathcal{V}_s \tag{22b}$$

$$\delta\ddot{\alpha}_{ij} = -\nu\dot{\alpha}_i - 2k\ \delta\alpha_{ij}, \qquad (i,j) \in \mathcal{E} \tag{22c}$$

where $\bar{\mathcal{M}}$ is defined as in Eq. (13), and $\delta\alpha_{ij}$ and $\delta\dot{\alpha}_{ij}$ represent the perturbations from the considered stable configuration of the target network, defined by $\alpha_{ij} = 0$ or 1 and $\ddot{\alpha}_{ij} = 0$ with $(i,j) \in \mathcal{E}$.

Equations (22a), (22b), and (22c) are decoupled, and therefore their stability can be studied separately. The linearized Eqs. (22b) and (22c) have negative eigenvalues and therefore are stable, while the stability of Eq. (22a) can be studied with the MSF approach summarized in Sec. III C 2.

By adopting strategy B, the steady-state topology of the network is selected from the set $\mathcal{K}$ of possible coupling configurations, which has cardinality

$$\frac{1}{2}\sum_{j=1}^{M} M!/j!(M-j)!,$$

where M is the number of possible network edges, defined by the set $\mathcal{E}$. Such configurations comprise all the combination of active and inactive coupling edges from $\mathcal{E}$.

Definition 4.1. Given the functional form of f and h and given the coupling and control gains σ and q, we denote by $\mathcal{PK}^*$ the (possibly empty) set of pinning and coupling configurations such that the master stability function Λ is negative.

We assume that, for the selected gains, $\mathcal{PK}^*$ is nonempty and we state the following theorem.

Theorem 4. *Consider a pinning and coupling configuration in* $\mathcal{PK}^*$. *For any local perturbation, the network in Eq. (4) is locally asymptotically controlled to the pinner trajectory and the snapping dynamics in Eq. (9), Eq. (20) are locally asymptotically stable.*

Proof. Following the same line of argument as in Theorem 1, the claim follows. □

Even though local stability properties of this strategy appear to be similar to the previous case, it is worth emphasizing that the decentralized adaptation of the network topology facilitates the synchronization process. In fact, the combined selection of the pinned nodes and of the steady-state topology of the target network expands the set of possible configurations of the controlled network. In this way, it is possible to drive the network towards a stable topological configuration even when this is impossible with strategy A. This concept is made clearer by the following numerical example.

A. Numerical validation

We analyze a network of 30 Rössler oscillators with state vector $x = [v,\ w,\ z]^T$ coupled through a scale-free like topology generated via the BA algorithm. The dynamics of the isolated Rössler oscillator can be written as

$$\begin{aligned}\dot{v} &= -w - z,\\ \dot{w} &= v - c_1 w,\\ \dot{z} &= c_2 + (v - c_3)z.\end{aligned}$$

By choosing the parameters as in Ref. 51, that is, $c_1 = c_2 = 0.2$ and $c_3 = 5.7$, the system exhibits chaotic behavior. We linearly couple the chaotic oscillators only through the variable v. Namely, $h(x) = \Gamma x$, where

$$\Gamma = \begin{bmatrix} 1 & 0 & 0 \\ 0 & 0 & 0 \\ 0 & 0 & 0 \end{bmatrix}.$$

Furthermore, the coupling gain σ is set to 0.15, the control gain q is set to 1, and $\mathcal{V}_s = \mathcal{V}$. The initial conditions for the node states are taken from a standard normal distribution; $a_{ij}(0)$ is se to 0 for $(i,j) \in \mathcal{E}$ and $\eta_i(0) = 0$ with $i \in \mathcal{E}$. As illustrated in Figure 3(a), strategy A is not able to fully control the network and a non-zero steady-state error remains. Therefore, even the activation of all the control gains, observed in Figure 4(a), does not guarantee the convergence of the network dynamics onto the trajectory of the pinner. In fact, the network topology is such that none of the possible pinning configurations is stable. Even in the case in which all nodes are pinned, Λ is still positive. On the other hand, through the snapping evolution reported in Figure 5, strategy B is able to drive the network into a locally pinning controllable region, that is, $\Lambda(\bar{\mathcal{M}}) < 0$, with the topology of the target network converging to a more homogeneous network, see Figure 6. Even though the steady-state target network topology is disconnected, as a result of the pinning selection process, see Figure 4(b), the disconnected nodes are directly

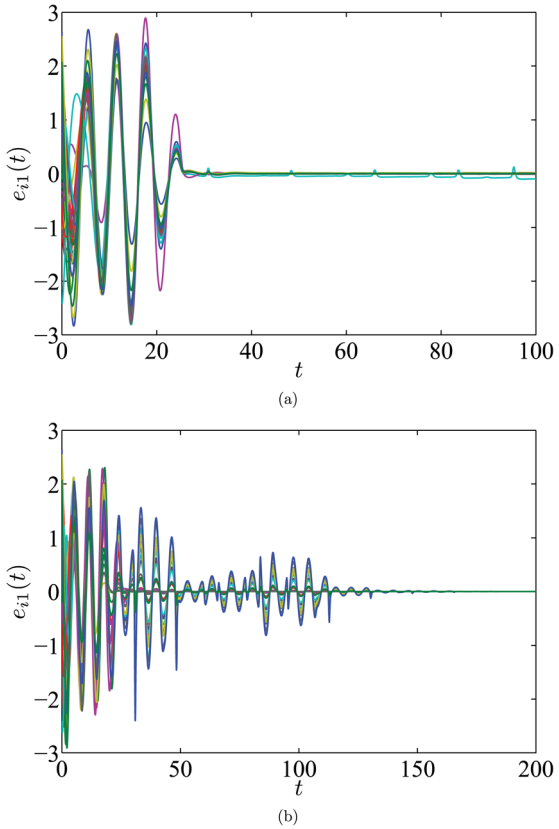

FIG. 3. (Color online) Pinning strategies A and B to control a network of 30 Rössler oscillators coupled on the variable v. strategy A is not able to completely control the network dynamics. A non-zero steady-state error remains (a). strategy B successfully controls the network (b).

controlled by the pinner to the desired trajectory. Moreover, notice that strategy B is more efficient as it allows for achieving a zero error, while the average degree of the steady-state topology of the target network is reduced from 6.3 to 2.1 when compared to the initial topology. While strategy A tries to pin all the 30 network nodes, only 15 are pinned when using strategy B, as illustrated in Figure 4.

V. FULLY DECENTRALIZED EDGE SNAPPING CONTROL

In the network Eq. (3), the coupling gain σ and the control gain q are selected offline as constant over time and common across the whole network nodes. This model may be inadequate to describe the controlled dynamics of a real network. In fact, real-world networks are often characterized by adaptive couplings which vary in time according to different environmental conditions. Such networks include wireless networks of sensors that gather and communicate data to a central base station[52,53] and neural networks that can adapt their synaptic connections.[54,55] In these cases, it is realistic to assume that the interactions are not identical across the network and time-varying.

For these reasons, according to Eq. (4), we propose to modify strategies A and B by introducing a fully decentralized control scheme of the form

$$\ddot{b}_i = -\zeta \dot{b}_i - \frac{\mathrm{d}}{\mathrm{d}b_i} U(b_i) + g(e_i), \qquad i \in \mathcal{V}_s, \qquad (23a)$$

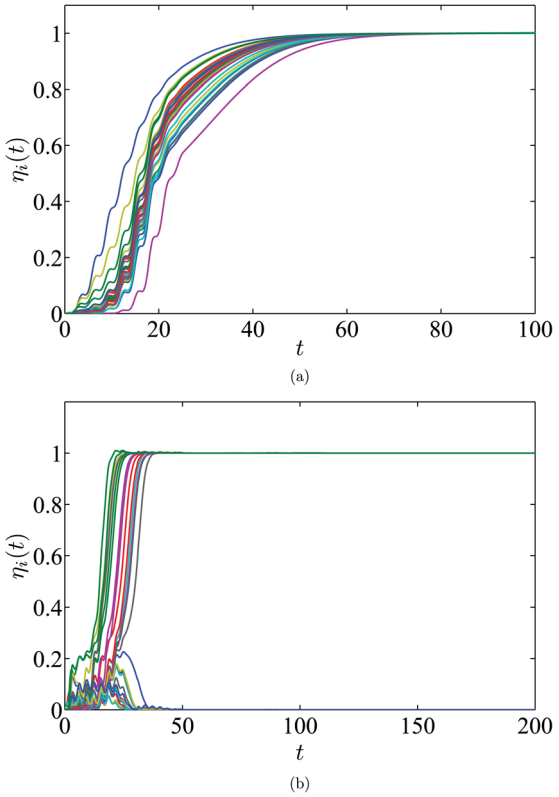

FIG. 4. (Color online) Pinning strategies A and B to control a network of 30 Rössler oscillators coupled on the variable p: selection of the pinning sites. When strategy A is adopted, all the pinning sites are activated at steady-state (a). When using strategy B, only half of the pinning sites are selected (b).

$$\ddot{\alpha}_{ij} = -\xi \dot{\alpha}_{ij} - \frac{\mathrm{d}}{\mathrm{d}\alpha_{ij}} U(\alpha_{ij}) + c(e_{ij}), \qquad (i,j) \in \mathcal{E}, \quad (23b)$$

$$\dot{q}_i = \eta_i e_i^T (h(x_i) - h(x_s)), \qquad i \in \mathcal{V}_s, \qquad (23c)$$

$$\dot{\sigma}_{ij} = a_{ij}(x_j - x_i)^T (h(x_j) - h(x_i)), \qquad (i,j) \in \mathcal{E}. \quad (23d)$$

Here, we assume $\sigma_{ij}(0) \geq 0$ with $(i,j) \in \mathcal{E}$ and $q_i(0) \geq 0$ with $i \in \mathcal{V}_s$, and we define the scalars a_{ij} with $(i,j) \in \mathcal{E}$ and η_i with $i \in \mathcal{V}_s$ as in Eqs. (19) and (8), respectively. The dynamics of the network nodes and of the pinner are described by Eq. (4); Eqs. (23a) and (23b) are the snapping dynamics determining the steady-state topology of the network and the

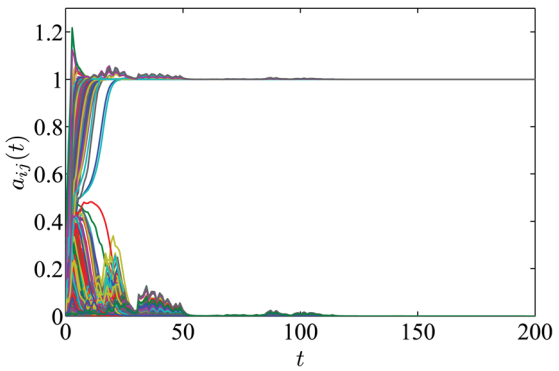

FIG. 5. (Color online) Network of 30 Rössler oscillators coupled on the variable v and controlled through strategy B. Snapping dynamics for the evolution of the network topology.

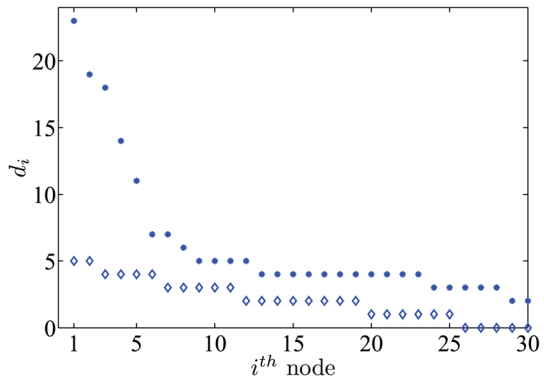

FIG. 6. (Color online) Control of a network of 30 Rossler oscillators coupled on the u variable via strategy B. Node degree for the target network before (stars) and after the evolution (diamonds) dictated by strategy B.

location of the pinned sites; Eqs. (23c) and (23d) allow for the modulation of the control and coupling gains.

The main advantage of this approach is that every aspect of the control scheme is adapted in a decentralized way: each pair of nodes in the controlled network can negotiate and decide whether activating or not their corresponding link and what should be the intensity of the coupling. In addition, the pinner adaptively selects the pinned nodes and the corresponding control gains.

To give a first insight into the effectiveness of the approach, we consider the same network analyzed in Figure 2. All initial conditions are set as before, the additional parameters $\sigma_{ij}(0)$ with $(i,j) \in \mathcal{E}$ and $q_i(0)$ with $i \in \mathcal{V}_s$ are selected to be zero. By comparing Figures 2 and 7, we find that the convergence to the desired trajectory is much faster with this fully decentralized approach, notwithstanding that the nodes of the target network are initially decoupled. Figure 8 demonstrates that all the coupling and control gains converge to steady-state values. Figure 9 illustrates the adaptive selection of the network edges and the pinned nodes.

We now provide a sufficient condition for stability of error dynamics and the convergence of the coupling and control gains.

Theorem 5. *If the vector field f is QUAD(Δ) with* $\Delta \leq \beta I_n < 0$, *and* $h(x) = \Gamma x$ *with* $\Gamma \geq 0$, *then*

- *The network in Eq. (23) is globally exponentially controlled to the desired trajectory described by Eq. (2).*

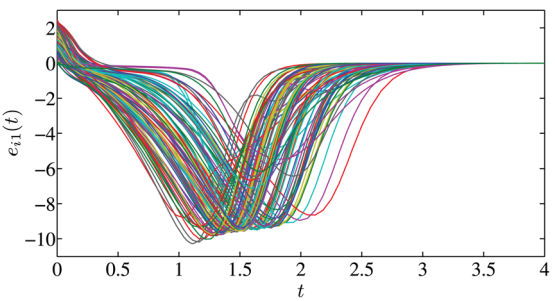

FIG. 7. (Color online) Network of 100 Lorenz oscillators with fully decentralized snapping control. Evolution of the first component of the pinning error.

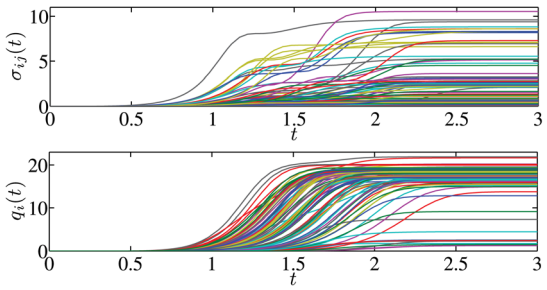

FIG. 8. (Color online) Network of 100 Lorenz oscillators with fully decentralized snapping control. Evolution of the coupling (top) and control gains (bottom).

- *All the coupling and control gains converge to finite steady-state values.*
- *The dynamics of the selection of the pinned sites described by Eq. (9) converges to an equilibrium configuration where nodes are either pinned or not.*
- *The evolution of the edges of the target network described by Eq. (20) converges to an equilibrium configuration.*

Proof. We organize the proof in three parts. First, we show that the error dynamics converges to zero. Then, we prove that the coupling and control gains converge to bounded values. Finally, we show that both the topology of the target network and the pinned sites' selection converge to an equilibrium configuration.

Convergence of the nodes onto the pinner trajectory can be proved by using Eq. (14) and following the same argument used to prove Theorem 2.

Now, consider the following candidate Lyapunov function:

$$V = \frac{1}{2} e^T e + \frac{1}{2} \sum_{(i,j)\in\mathcal{E}} (\sigma_{ij} - \bar{\sigma}_{ij})^2 + \frac{1}{2} \sum_{i\in\mathcal{V}_s} (q_i - \bar{q}_i)^2, \qquad (24)$$

where $\bar{\sigma}_{ij}$ with $(i,j) \in \mathcal{E}$ and $\bar{q}_i$ with $i \in \mathcal{V}_s$ are the nonnegative unknown steady-state coupling and control gains, respectively. The derivative of V along the trajectories of the network can be written as

$$\dot{V} = e^T \dot{e} + \sum_{(i,j)\in\mathcal{E}} (\sigma_{ij} - \bar{\sigma}_{ij}) \dot{\sigma}_{ij} + \sum_{i\in\mathcal{V}_s} (q_i - \bar{q}_i) \dot{q}_i. \qquad (25)$$

From Eqs. (23c) and (23d) and recalling that the function f is QUAD with $\Delta \leq \beta I_n < 0$ and that $h(x) = \Gamma x$, we can write

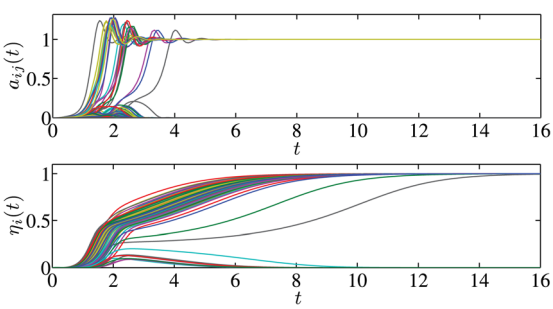

FIG. 9. (Color online) Network of 100 Lorenz oscillators with fully decentralized snapping control. Evolution of a_{ij} (top) and δ_i (bottom).

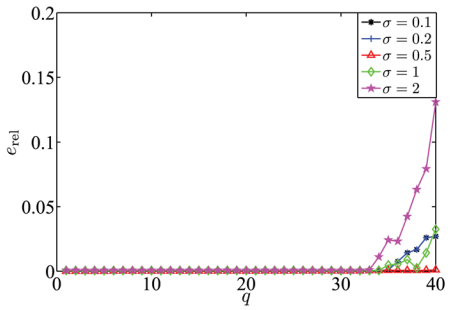

(a) Steady-state error e_{rel} versus the control gain q.

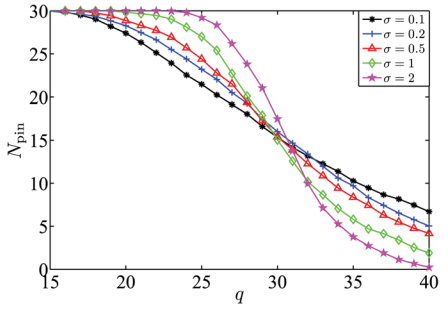

(b) Number N_{pin} of pinned nodes at steady-state versus the control gain q.

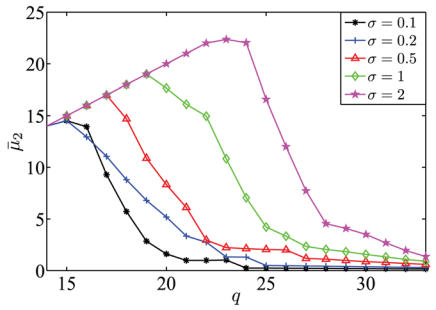

(c) $\bar{\mu}_2$ versus the control gain q.

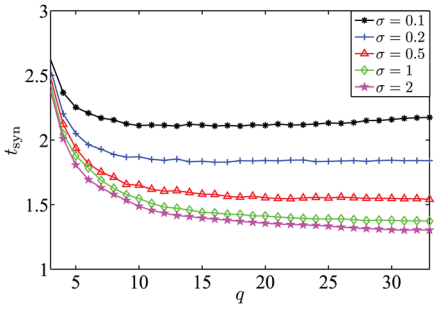

(d) Time of synchronization t_{syn} versus the control gain q.

FIG. 10. (Color online) Control of a network of 30 Chua's circuits through strategy A.

$$\dot{V} = e^T(I_N \otimes \Delta)e + \sum_{(i,j)\in\mathcal{E}} a_{ij}\sigma_{ij}e_i^T\Gamma(e_j - e_i) - \sum_{i\in\mathcal{V}_s}\eta_i q_i e_i^T\Gamma e_i + \sum_{(i,j)\in\mathcal{E}}(\sigma_{ij} - \bar{\sigma}_{ij})a_{ij}(e_j - e_i)^T\Gamma(e_j - e_i) + \sum_{i\in\mathcal{V}_s}(q_i - \bar{q}_i)\eta_i e_i^T\Gamma e_i. \tag{26}$$

Notice that $\sum_{(i,j)\in\mathcal{E}} \sigma_{ij}a_{ij}e_l^T\Gamma(e_j - e_i)$ can be written as

$$-\sum_{(i,j)\in\mathcal{E}} \sigma_{ij}a_{ij}(e_j - e_i)^T\Gamma(e_j - e_i).$$

Hence, from Eq. (26) we have

$$\dot{V} \le e^T(I_N \otimes \Delta)e - \sum_{(i,j)\in\mathcal{E}} \bar{\sigma}_{ij}a_{ij}(e_j - e_i)^T\Gamma(e_j - e_i) - \sum_{i\in\mathcal{V}_s}\bar{q}_i\eta_i e_i^T\Gamma e_i. \tag{27}$$

Since $\Gamma \ge 0$ and $\Delta \le \beta I_n$ by hypothesis, we finally obtain

$$\dot{V} = \beta e^T e, \tag{28}$$

which implies that $\dot{V} \le 0$ for all e, σ, q. Therefore, we conclude that all the elements of σ and q are bounded. Furthermore, from Eqs. (23c) and (23d) and the fact that $\Gamma \ge 0$, both the coupling and control gains are non-decreasing. Then, we can conclude that they converge to finite steady-state values.

The convergence of the topologies of the target network and of the dynamics of the pinning sites selection can be shown following the same line of argument as in Theorem 2. In fact, both Eqs. (23a) and (23b) can be viewed as a Duffing-Holmes equations subject to a bounded and asymptotically vanishing input, since both e_i and $e_i - e_j$ are bounded and vanish exponentially, for all $i,j = 1,\ldots,N$. □

VI. DISCUSSION

Here, we compare the performance of all the proposed pinning control strategies. As a reference example, we consider a network of 30 Chua's circuits coupled through a scale-free like topology with average degree $\bar{d} = 6.4$, but similar considerations can be drawn for different node dynamics, network size, and target network topology. The results of our numerical experiments are averaged over 50 repetitions, in which different initial conditions, selected randomly from a normal distribution, are considered. In all the simulations we set $\mathcal{V}_s = \mathcal{V}$ and $\eta_i(0) = 0$ for $i \in \mathcal{V}_s$.

To characterize the speed of convergence, we define the synchronization time t_{syn} as the first time instant such that the error norm remains bounded by a given constant. Namely,

$$t_{syn} = \min t \quad \text{such that } ||e(t)|| \le 0.01, \quad \forall t \ge t_{syn}. \tag{29}$$

To further evaluate the performance of the proposed schemes, we introduce the following parameter:

$$e_{rel} = \frac{\bar{e}}{||e(0)||}, \tag{30}$$

where

$$\bar{e} = \frac{1}{t_2 - t_1}\int_{t_1}^{t_2} ||e(t)||\mathrm{d}t,$$

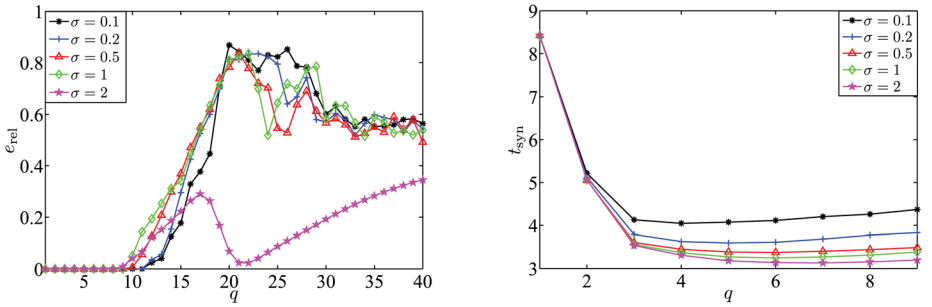

(a) Steady-state error e_{rel} versus the control gain q.

(b) Time of synchronization t_{syn} versus the control gain q.

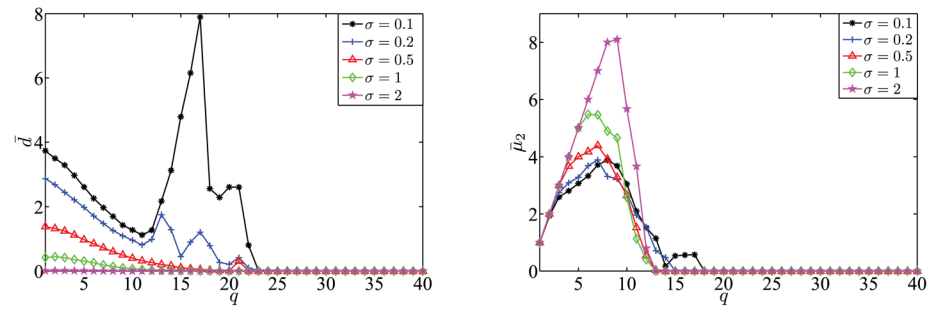

(c) Average degree $\bar{d}$ of the emerging target network topology versus the control gain q.

(d) $\bar{\mu}_2$ versus the control gain q.

FIG. 11. (Color online) Control of a network of 30 Chua's circuits through strategy B.

and $t_1, t_2 \gg t_{\text{syn}}$ are equal to 90 and 100, respectively. These values are heuristically selected to assure synchronization of the coupled chaotic systems as well as to capture time variations within the averaging window $[t_1, t_2]$.

In Figure 10, the performance of strategy A is summarized, for values of σ ranging from 0.1 to 2 and for a coupling gain q between 1 and 40. Figure 11 shows that synchronization is achieved for all the coupling gains if $q \leq 33$. For higher control gains, the error norm always remains bounded, but controlled synchronization is achieved only for $0.2 \leq \sigma \leq 0.5$. When the network synchronizes onto the pinner trajectory, the selection of the gains has a clear influence on the performance of the control strategy. In fact, as the control gain is increased, there is a transition from the case in which all the nodes are pinned at steady-state to the case where very few nodes are pinned. This transition is faster as the coupling gain increases, see Figure 10(b). At steady-state, a pinning configuration is always achieved. Notice that its second smallest eigenvalue $\bar{\mu}_2$ initially increases as the control gain is increased, reaches global maximum, and then decreases. Moreover, the maximum value attained by $\bar{\mu}_2$ increases with the coupling gain σ, see Figure 10(c). The synchronization time is reduced as the control gain is increased, except for σ lower than 0.2. In this case, after an initial reduction, increasing q leads to an unchanged or slightly increased synchronization time, as depicted in Figure 10(d).

In the numerical analysis of strategy B, we set $a_{ij}(0) = 0$ for $(i, j) \in \mathcal{E}$. In Figures 11 and 12, the performance of strategy B is summarized, for values of σ ranging from 0.1 to 2 and for a coupling gain q between 1 and 40. As illustrated, the performance of the proposed strategy is very sensitive to the choice of the coupling and control gains. In fact, when the control gain is higher than 15, synchronization is rarely achieved while the error norm remains bounded, see Figure 11(a). The network topological evolution never reaches a steady-state, continuing to oscillate about unstable configurations. In particular, for $q \geq 25$, the snapping dynamics is not able to activate any pinning gain and controlled synchronization is not feasible, see Figures 12.

It is worth emphasizing that a bounded synchronization is always guaranteed with both strategies A and B. Nonetheless, the problem of tuning the coupling and control gains appears to be crucial in optimizing the control performance. On the contrary, strategy C does not require any tuning. In fact, it is able to adaptively tune the coupling and control gains that in our simulation are set to 0 at the onset of the evolution. From the numerical analysis, it is evident that the performance of strategy C is remarkably superior to the performance of the first two strategies. Specifically, with this approach, controlled synchronization is always achieved. Furthermore, we observe that the synchronization time $t_{\text{syn}} = 2.32$ is significantly reduced as compared to strategy B while it is comparable to synchronization times achieved through strategy A. The latter result is more surprising considering that, differently from strategy A, at the onset of the evolution the controlled network is completely disconnected. Furthermore, this fast convergence is obtained with an emerging target network with average degree of 1.98, that is, a much sparser network when compared to the target networks emerging from strategy B and to the static network of strategy A. The improved performance of this strategy is due to the decentralized adaptive selection of the coupling and control gains, which in our numerical experiments are on average 18.64 and 3.52, respectively.

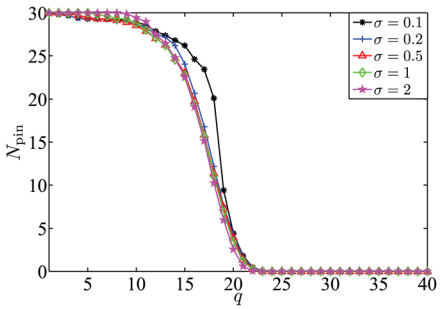

(a) Number N_{pin} of pinned nodes at steady-state versus the control gain q.

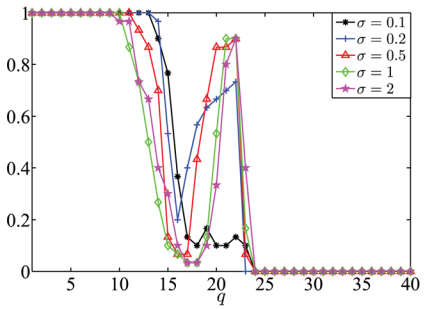

(b) Fraction of experiments in which synchronization is reached in less than 100 seconds versus the control gain q.

FIG. 12. (Color online) Control of a network of 30 Chua's circuits through strategy B.

VII. CONCLUSIONS

In this paper, we presented three novel adaptive pinning control schemes for controlled synchronization of networks based on edge snapping. These pinning strategies address the fundamental need in pinning control schemes of selecting the sites to pin in a completely decentralized and adaptive way. This avoids the need of an off-line tuning of the pinning parameters. In particular, the first pinning strategy addresses the selection of pinned sites in networks with a static target topology. In the second strategy, controlled evolution of the target topology is considered to better control nodes' dynamics. The third strategy combines the adaptive selection of the pinned sites and of the topology of the target network with the decentralized adaptation of both the coupling and control gains.

We performed local and global stability analysis showing the viability of the proposed approach. Furthermore, we numerically assessed the effectiveness of this approach with fixed and adaptive control gains, highlighting the strong performance improvement that can be achieved when coupling and control gains are simultaneously adapted. The performance analysis suggests that a fully decentralized adaptation scheme, that is able to adaptively evolve the steady-state network topology and tune the strength of the interaction between each nodes' pairs, is preferable against methods based on static networks. Simulation results show that global controllability is actually possible for a wide class of node dynamics for which QUAD conditions may not be verified and yet local synchronization conditions presented in this paper apply. Therefore, a pressing open problem for future work is to relax the QUAD condition required to prove global stability of the network dynamics. This is the subject of ongoing work.

ACKNOWLEDGMENTS

This work was supported in part by the National Science Foundation under Grant CMMI-0745753 and in part by the University of Naples Federico II.

[1]N. Jeong, B. Tombor, R. Albert, Z. N. Oltval, and A. Barabási, Nature **407**, 651 (2000).
[2]S. Eubank, H. Guclu, V. S. A. Kumar, M. V. Marathe, A. Srinivasan, Z. Toroczkai, and N. Wang Nature **429**, 180 (2004).
[3]J. H. Fowler, and N. A. Christaki, Br. Med. J. **337**, a2338 (2008).
[4]J. Semmler, Exerc Sport Sci. Rev. **30**, 8 (2002).
[5]S. Boccaletti, V. Latora, Y. Moreno, M. Chavez and D. U. Hwang, Phys. Rep. **424**, 175 (2006).
[6]M. E. J. Newman, SIAM Rev. **45**, 167 (2003).
[7]M. E. J. Newman, A. L. Barabàsi, and D. J. Watts, *The Structure and Dynamics of Complex Networks* (Princeton University Press, Princeton, NJ, 2006).
[8]G. V. Osipov, J. Kurths, and C. Zhou *Synchronization in Oscillatory Networks* (Springer, Berlin, Germany, 2007).
[9]A. Pikovsky, M. Rosenblum, and J. Kurths *Synchronization: A Universal Concept in Nonlinear Science* (Cambridge University Press, Cambridge, UK, 2001).
[10]M. Rabinovich, H. Abarbanel, R. Huerta, R. Elson, and A. Selverston, IEEE Trans. Circuits Syst., I **44**, 997 (1997).
[11]T. Yang, C. W. Wu, and L. Chua, IEEE Trans. Circuits Syst., I **44**, 469 (1997).
[12]J. Gonzalez-Miranda, *Synchronization and Control of Chaos* (Imperial College Press, London, UK, 2004).
[13]R. O. Grigoriev, M. C. Cross, and H. G. Schuster, Phys. Rev. Lett. **79**, 2795 (1997).
[14]T. Chen, X. Liu, and W. Lu, IEEE Trans. Circuits Syst., I **54**, 1317 (2007).
[15]M. Porfiri and M. di Bernardo, Automatica **44**, 3100 (2008).
[16]M. Porfiri and F. Fiorilli, Physica D **239**, 454 (2010).
[17]H. Yang, Z. Zhang, and S. Zhang, Int. J. Robust Nonlinear Control **21**, 945 (2011).
[18]M. Porfiri and F. Fiorilli, Chaos **19**, 013122 (2009).
[19]X. Li, X. Wang, and G. Chen, IEEE Trans. Circuits Syst., I **51**, 2074 (2004).
[20]F. Sorrentino, M. diBernardo, F. Garofalo, and G. Chen, Phys. Rev. E **75**, 046103 (2007).
[21]J. Zhou, J.-A. Lu, and J. Lu, Automatica **44**, 996 (2008).
[22]W. Yu, G. Chen, and J. Lü, Automatica **45**, 429 (2009).
[23]P. DeLellis, M. diBernardo, F. Garofalo, and M. Porfiri, IEEE Trans. Circuits Syst., I **57**, 2132 (2010).
[24]L. Wang, H. Dai, X. Kong, and Y. Sun, Int. J. Robust Nonlinear Control **19**, 495 (2009).
[25]Y.-W. Wang, J.-W. Xiao and H. O. Wang, Int. J. Robust Nonlinear Control **20**, 1667 (2010).
[26]X. F. Wang and G. Chen, Int. J. Bifurcation Chaos **12**, 187 (2002).
[27]C. Li, L. Chen and K. Aihara, Phys. Biol. **3**, 37 (2006).
[28]J. Zhou and T. Chen, IEEE Trans. Circuits Syst., I **53**, 733 (2006).
[29]J. Lü, X. Yu, G. Chen and D. Cheng, IEEE Trans. Circuits Syst., I **51**, 787 (2004).
[30]T. Balch and R. C. Arkin, IEEE Trans. Rob. Autom. **14**, 926 (1998).
[31]R. W. Beard, A. W. Beard, J. Lawton and F. Y. Hadaegh, IEEE Trans. Control Syst. Technol. **9**, 777 (1999).
[32]A. Das, R. Fierro, V. Kumar, J. Ostrowski, J. Spletzer and C. Taylor, IEEE Trans. Rob. Autom. **18**, 813 (2002).
[33]W. Ren and E. Atkins "Distributed multi-vehicle coordinated control via local information exchange," International Journal of Robust and Nonlinear Control **17**, 1002 (2007).
[34]G. Wen, Z. Duan, W. Yu, and G. Chen, Int. J. Robust Nonlinear Control **21**, n/a (2011).
[35]P. DeLellis, M. diBernardo and F. Garofalo, Chaos **18**, 037110 (2008).

[36]P. DeLellis, M. diBernardo and F. Garofalo, Automatica **45**, 1312 (2009).
[37]H. K. Khalil, *Nonlinear systems*, 3rd ed. (Prentice Hall, Englewood Cliffs, NJ, 2002).
[38]P. DeLellis, M. di Bernardo, and G. Russo, IEEE Trans. Circuits Syst., I **58**, 576 (2011).
[39]W. Lohmiller and J. Slotine, Automatica **34**, 683 (1998).
[40]W. Lohmiller and J. J. E. Slotine, AIChE J. **46**, 588 (2000).
[41]D. D. Siljak, Nonlinear Anal.: Hybrid Syst. **2**, 544 (2008).
[42]R. Merris, Linear Algebr. Appl. **197-198**, 143 (1994).
[43]T. Nishikawa and A. E. Motter, Physica D **224**, 77 (2006).
[44]P. Holmes, Philos. Trans. R Soc. London, Ser. A **292**, 419 (1979).
[45]P. Bartissol and L. O. Chua, IEEE Trans. Circuits Syst. **35**, 1512 (1988).
[46]A. Barabàsi, R. Albert, and H. Yeong, Physica A **281**, 69 (2000).
[47]E. N. Lorenz, J. Atmos. Sci. **20**, 130 (1963).
[48]E. Ott *Chaos in Dynamical Systems* (Cambridge University Press, Cambridge, UK, 1993).
[49]S. H. Strogatz, *Nonlinear Dynamics and Chaos* (Perseus Publishing, Cambridge, Massachussets, 1994).
[50]P. Erdös and A. Rényi, Publication of the Mathematical Institute of the Hungarian Academy of Sciences **5**, 17 (1960).
[51]O. E. Rössler, Phys. Lett. A **57**, 397 (1976).
[52]A. Cerpa and D. Estrin, IEEE Trans. Mobile Comput. **3**, 272 (2004).
[53]J.-M. Chen, J.-J. Lu and Q.-H. Wang "Research and improvement of adaptive topology algorithm leach for wireless sensor network," in *Proceedings of the 4th International Conference on Wireless Communications, Networking and Mobile Computing, WiCOM'08*, Dalian, 12-14 October 2008, pp. 1–4.
[54]P. Mazzoni, R. A. Andersen, and M. I. Jordan, Proc. Natl. Acad. Sci. U. S. A. **88**, 4433 (1991).
[55]M. Gupta and D. Rao, Fuzzy Sets Syst. **61**, 1 (1994).